International Journal of Geosciences, 2026, 17(3), 162-182
https://www.scirp.org/journal/ijg
ISSN Online: 2156-8367
ISSN Print: 2156-8359

Gold Mineralization Targets in Dang-Patou Zone: Metallotectic Context of the Gold-Bearing Zone (Betare-Oya, East Cameroon)

Ntoumbé Mama[1*], Ntieche Benjamin[2], Mounjouohou Aziz[3], Amaya Adama[4], Nchare Mominou[5], Ndang Vanisa[1], Guihdama Dagwai[6], Ngounouno Ismaïla[7]

[1]Department of Mining Geology, School of Geology and Mining Engineering, University of Ngaoundere, Meiganga, Cameroon
[2]Geology Laboratory, Higher Teacher Training College, University of Yaoundé 1, Yaoundé, Cameroon
[3]Department of Mineral Engineering, Chemical Engineering and Mineral Industry, University of Ngaoundere, Meiganga, Cameroon
[4]Department of Geomatic and Geology Mapping, School of Geology and Mining Engineering, University of Ngaoundere, Meiganga, Cameroon
[5]Department of Mineral Processing, School of Geology and Mining Engineering, University of Ngaoundere, Meiganga, Cameroon
[6]Department of Earth Science and Life, Higher Teacher Training College, University of Maroua, Maroua, Cameroon
[7]Department of Earth Sciences, Faculty of Sciences, University of Ngaoundere, Ngaoundere, Cameroon
Email: *ntoumbemama@gmail.com, ntoumbe2@hotmail.com

How to cite this paper: Mama, N., Benjamin, N., Aziz, M., Adama, A., Mominou, N., Vanisa, N., Dagwai, G. and Ismaïla, N. (2026) Gold Mineralization Targets in Dang-Patou Zone: Metallotectic Context of the Gold-Bearing Zone (Betare-Oya, East Cameroon). *International Journal of Geosciences*, **17**, 162-182.
https://doi.org/10.4236/ijg.2026.173009

Received: September 1, 2025
Accepted: March 23, 2026
Published: March 26, 2026

Abstract

The search of mineral resources and potential mineralization zones is one of the most demanding activities in the mining domain. This activity requires the use of appropriate methods that can provide accurate information about the geology of the desired area. Mineral exploration has greatly improved over the last years with the innovation of advanced techniques such as remote sensing. Satellite data is an important source of geological information for litho-structural mapping and mineral exploration. The studies carried out in the zone of Dang-Patou and surroundings focus on understanding the metallotectonic context of the zone using field data and satellite imagery. The analysis revealed a correlation between surface morphology and deep structural features, characterized by a significant concentration of intrusive bodies. The study area is made up of plutonic, sedimentary, and metamorphic rocks. Several geological criteria for gold mineralization, such as Banded Iron Formation (BIF), Quartz veins, Major Faults, and Dykes, are present in the study area. A potential mineralization map of the study area was realized, indicating points with a high degree of mineral concentration and this was confirmed by plotting some coordinate points obtained in the field on the map. This study will enable mineral explorers to target their exploration more effectively, ensure they are using the right exploration tools, and make more objective management decisions while quickly moving closer toward finding an ore deposit. Satellite im-

agery, geological mapping, and field investigations were utilized to identify lineaments corresponding to major tectonic faults associated with numerous small-scale deposits and ore occurrences. The exploration of gold and other minerals has identified known areas and several new localities for mineral resource/mineralization investigation.

Keywords

Metallotectic Context, Gold Mineralization, Fluid Flow, Field Data, Satellite Imagery, Dang-Patou

1. Introduction

Dang-Patou area is situated in the East region of Cameroon precisely Lom and Djerem Division and Betare-Oya District. Betare Oya is underlain by a series of granitic rocks, including granodiorite and tonalite, that are locally cut by systems of gold-bearing quartz veins (**Figure 1**) [1] [2]. This zone can be reached through Mararaba from Betare-Oya or Mabele through Beka-Guiwang. It is also accessed by following the 271 km road from Meidougou (**Figure 2**). The metallotectic

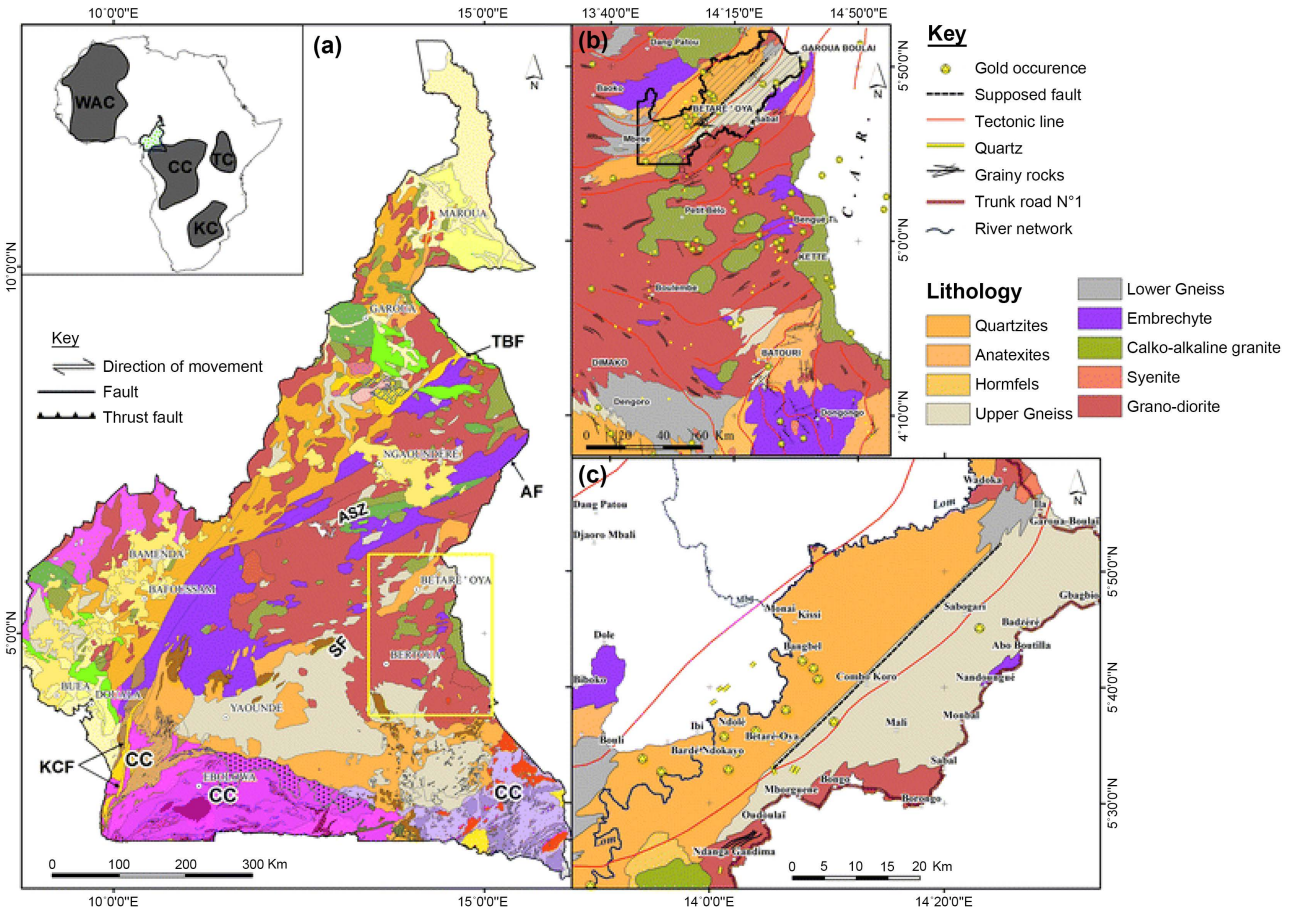

Figure 1. Geological map of Cameroon, modified [2].

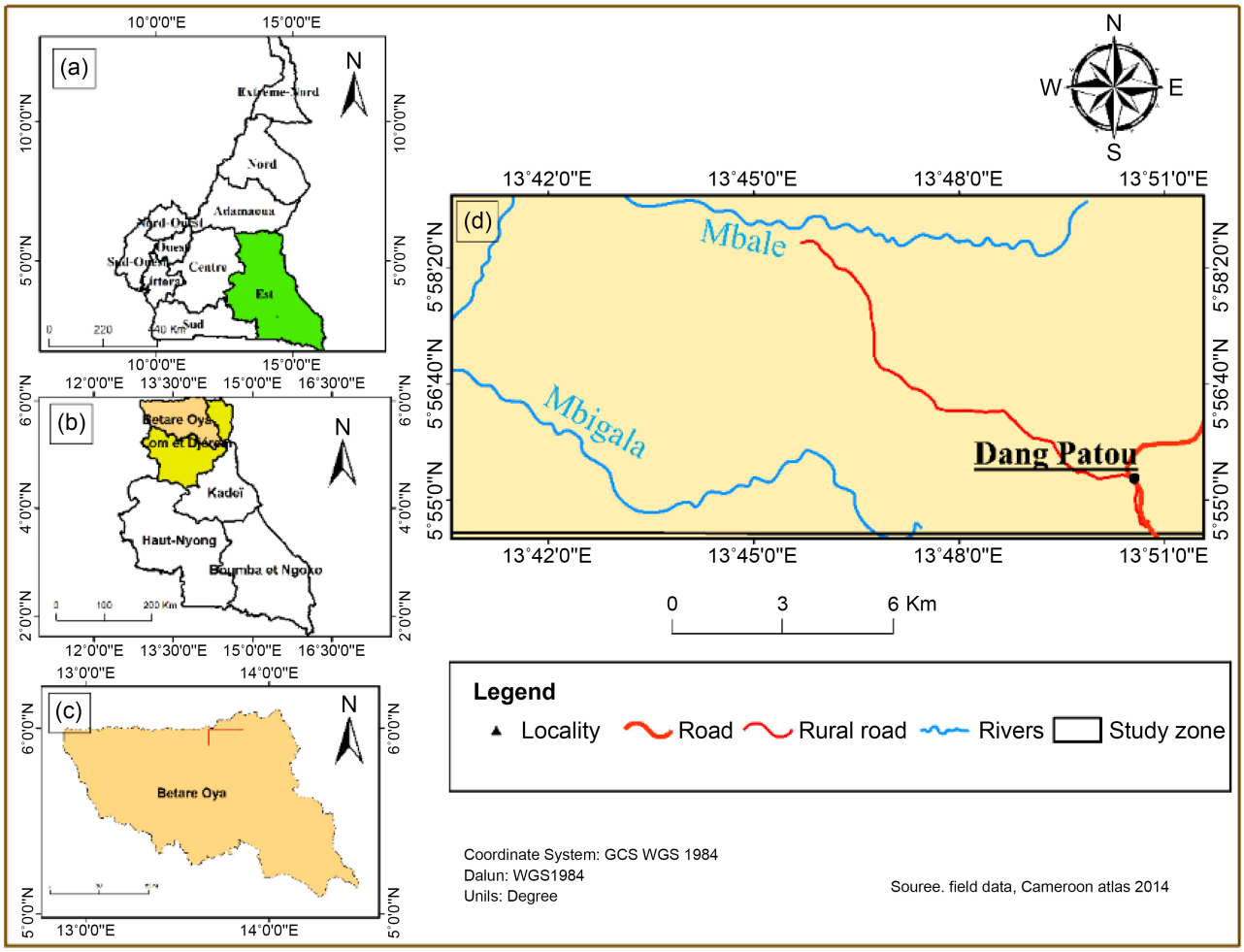

Figure 2. Location map of Dang-Patou (a) East region; (b) Lom and Djerem division, Betare-Oya district; (c) Betare-Oya district; (d) study zone.

context of an auriferous zone refers to the metallogenic factors that contribute to the formation and distribution of gold deposits and crucial for exploration [3]. These ore-forming processes are identified from existing literature about the mineralization system [4]-[6] and spatially using GIS analysis to predict mineral potential in the study region. Mineral deposit locations for hard rock gold mineralization were extracted from the GERM mineral deposit database [7]. Alluvial or eluvial gold deposits can have various sources, and involves studying the processes that led to the mineralization of the gold [8]. The primary Au ore is hosted in the biotite and muscovite granite and occurs mostly as structurally controlled (veins, veinlets and stockwork) and locally disseminated ore. The structure of mineralization gold, the mineral assemblage, the host rock composition, and the geodynamic setting of Adamawa region and particularly around Meiganga area are presented [9]. Several geological criteria for gold mineralization were compiled from different references [10]-[14] that appear to be suitable for this area, such as Banded Iron Formation (BIF), Quartz veins, Major Faults, and Dykes. These gold deposits are typically found in river beds, flood plains and other areas where water flow has

transported and concentrated gold particles from their primary sources. Satellite remote sensing images have been widely and successfully used for mineral exploration since the launch of Landsat in 1972 [15] [16]. Many ore deposits have been recognized using satellite imagery [17]-[19]. This paper provides further information on the location of potential mineralization zones of the Dang-Patou area using field data and remote sensing techniques to identify mineral resources. Moreover, it presents the lithologic types of the study area and uses the simple image processing methods to do the geological mapping of gold deposits and other mineralization. This includes the mineralogy, structural geology, and remote sensing data recording information based on material composition and the analysis of many geological features essential for the gold exploration.

2. Geological Setting

The eastern region of Cameroon is characterized by significant gold mining activities. The most dominant area of shearing is situated along the contact between undated high-grade migmatitic gneisses and schists, and the eastern edge of the Lom Belt defined by the Betare-Oya Shear Zone [20]. Some veins cut the Neoproterozoic metavolcanic-metasedimentary rocks, undated older metamorphic rocks, and the Pan-African plutonic rocks, but other auriferous veins occur along the contact between rock layers [21]-[24] and [25]. The rocks of the Lower Lom Belt can be grouped into three categories based on their structure and mineralogy, with gold occurring in all three types of rock, ranging from the edges to the middle of the belt. Veins are most commonly composed of hydrothermal minerals such as quartz, carbonates, chlorite, muscovite, sulfides, and/or tellurides [26]. These include chlorite-sericite schist, which is linked to the edges of the ductile to brittle shear zones and includes the Betare-Oya Shear Zone. The chlorite-sericite schists are strongly deformed, with interbedded quartz veins displaying pinch-and-swell and shearing features, which appear to represent Riedel structures related to the main shear zone. The schistosity generally has a high to moderate northwesterly dip. The mineralogical composition of the schist is dominated by quartz, ilmenite, rutile, zircon, pyrite, muscovite, sericite, and staurolite. Garnet, magnetite/hematite, and graphite have also been identified in this region. The Betare Oya area is part of the Neoproterozoic (700 - 1100 Ma) volcano-sedimentary formations of Cameroon or schist belts, which are also known as the Lower Lom series. These rock formations can be found on top of the Pan-African basement, which is made up of migmatite and granitic to orthogneissic, biotite-rich rocks. These rock formations are found in the NE-SW trending shear zones as part of the Central African and Cameroon shear zone [27]. The Betare Oya gold field is found within a major shear zone that represents extensions along the Sanaga fault line. This structure is found in the valleys formed when rock blocks are moved along faults and bears a resemblance to other basins that have been formed by rock blocks moving along faults [28]. It is hypothesized that the basin was filled with eroded and transported materials from N30E-N40-E striking gold-bearing quartz veins [29] [30]

and slightly changed quartzites and granitoids.

3. Methodology

3.1. Fundamentals of Remote Sensing in Mineral Exploration

Data acquired from field campaigns, laboratory analyses, and remotely sensed imagery were processed using specialized software, including Basecamp, ArcGIS 10.5, Geomatica, Envi 4.7, and GeoRose. Remote sensing is defined as the science of acquiring, preparing, and interpreting spectral and spatio-temporal information about a target—be it an object, area, or phenomenon—without direct physical contact. This transfer of information is facilitated by electromagnetic radiation (EMR), a form of energy detectable by its observable effects upon interaction with matter [16].

In geological applications, spectral imaging is a powerful tool for detecting mineral resources. Distinct spectral signatures of rocks and alteration minerals can be used to identify areas favorable for mineral deposits, thereby significantly reducing the time and cost associated with traditional exploration programs [31]. Satellite imagery, particularly from the Landsat program, has been extensively employed to generate base geological maps and to detect hydrothermal alteration zones that are often associated with ore deposits [32]. Furthermore, these images are effective for mapping structural features such as faults, fractures, and lineaments, which can provide critical clues to the location of concealed mineralization [33].

3.2. Remote Sensing Methodology

A spatial correlation analysis was conducted using themes relevant to mineral prospectivity, including structural geology, lithology, stratigraphy, hydrothermal alteration, geochemistry, and geophysics, as outlined by [7]. Structural features were analyzed using a buffering methodology described by [34] to determine the optimal spatial proximity for the greatest number of mineral prospects relative to these features. Individual faults were also analyzed in combination to test their collective relationship with mineralization.

Remote sensing is particularly advantageous for mineral exploration as it enables the systematic collection of digital data over large and often inaccessible areas. It serves as a robust tool for providing high-resolution image data and enabling reliable geological mapping during the preliminary stages of exploration. A key application is the extraction of lineaments to target hydrothermally altered zones for gold exploration. This technique has been successfully applied in the Pan-African belt of Cameroon to identify hydrothermal alteration and numerous mineralization-associated lineaments. Integrating remote sensing with field data significantly improves the targeting of potential primary gold resources within hydrothermal and structural systems, allowing for the precise localization and mapping of geological structures [35].

For this study, a Landsat 8 Operational Land Imager (OLI) and Thermal Infrared Sensor (TIRS) image was selected to map mineral distribution. The OLI sensor comprises bands 1 - 7 and 9, while the TIRS sensor consists of bands 10 and 11;

band 8 is a panchromatic band. The satellite image underwent pre-treatment techniques followed by specialized image processing. The spectral characteristics of the Landsat sensors are detailed in [36] and [37].

Lineaments are defined as linear geological features or alignments of features, topographic discontinuities, or geomorphological elements inherited from paleotopographies [38]. They are critical for inferring mineral prospects, analyzing deformation patterns, identifying geological boundaries, and interpreting subsurface structures in areas with limited exposure [39]. Lineament extraction can be performed through two primary approaches: manual extraction based on visual interpretation and an interpreter's knowledge [40], and automatic extraction utilizing computer algorithms [41]. The automated process typically involves edge detection, thresholding, and curve extraction [42] and [43]. Edge enhancement techniques were applied to delineate features and accentuate shapes and details within the image. Automatic extraction was performed by selecting the optimal spectral band from the Landsat 8 image to best identify linear features across the study area. The integration of geographic information Systhem (SIG) in the exploration of gold mineralization at Ndang Patou is synthesized in **Figure 3**. This figure details the methodological stage involved in developing predictive metallogenic mapping.

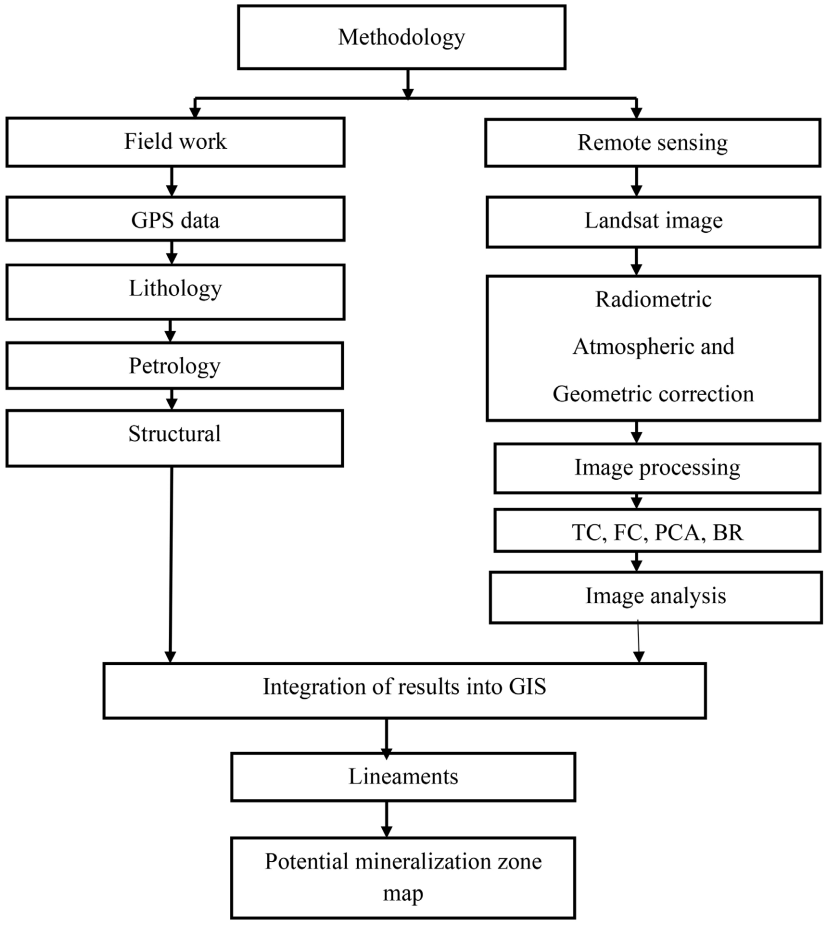

Figure 3. Flowchart of remote sensing and field studies.

3.3. Sampling Techniques, Petrographic, and Structural Analysis

The collected dataset was integral to understanding the source of mineralization and identifying potential target zones within the study area. Analysis of topographic maps and field observations focusing on rock color, degree of alteration, morphology, and structural elements led to the identification of numerous quartz veins and pegmatite bodies.

Structural measurements, including the strike and dip of planar features and the dimensions of veins, were acquired using standard geological methods. The right-hand rule convention was employed for strike and dip data collection. Representative rock samples were collected using a geologic hammer for subsequent petrographic thin section preparation. Macroscopic sample descriptions were based on structure, color, grain size, visible mineralization, and fossil content. The orientation and distribution of quartz veins, which are commonly associated with faults and fractures, provide valuable insights into the tectonic history and deformation processes that have affected the region.

4. Results

4.1. Soil Profiles

The ferralitic soils are lateritic or made up of gravel and are poor in nutritive elements. They are low in silica and high in iron minerals because of weathering. Primary minerals are mostly absent in these soils except for quartz, which does not undergo weathering (**Figure 4**). The dominant secondary minerals found in these soils are a combination of gibbsite, goethite, and hematite. Hydromorphic soils are formed in the presence of excess moisture. They are found in marrecageous valleys. They present sand deposits in certain areas or laterites. The depths at which the samples were collected were dictated by the various regolith profiles (**Figures 4(a)-(c)**). Soil profiles are characterized by numerous horizons (O, A, B, and C). The dark brown sandy clay layer of the study area is marked by the presence of plant roots (horizon O) and organic matter decomposition. From the profile shown in **Figure 4(c)**, the preserved surface is characterized by landscape modification which does not introduce any foreign regolith material that may cause dilution or enhancement of Au. The horizon A shows less organic matter and small quantities of clay with medium to fine grain clay sand. Horizon B is dominated by the accumulation of clay and small particles of sand with a whitish brown color. Horizon C presents a layer rich in sandy clay with a grain particle size ranging from 0.06 mm to 2 mm. Apart from the mineralized sand layer, the horizon consisted of quartz, feldspars, and mica, sand pyrite, chalcopyrite, sphalerite, and gold. The detrital types occur generally in areas where quartz veins are associated with the underlying bedrock. This horizon has some rounded quartz fragments, boulders of older duricrust as well as rock boulders and floats of varying origin, all packed up in seemingly the same horizon. Pyrite is the most abundant sulfide mineral with a pale brass yellow color giving a superficial resemblance to gold (**Figure 5(a)**).

Pyrite crystals sometimes contain occasional particles of real gold that were trapped up during the crystallization process (Figure 5(b)). The bleached zone stands as a major indicator of hydrothermal alteration, even though it usually does not contain Au. These minerals are extracted from secondary deposits that are connected to quartz veins that intrude plutonic bedrocks. The surface deposits comprise colluvial material derived from the bordering hills. These deposits exhibit evidence of limited transport and are locally cemented by caliche.

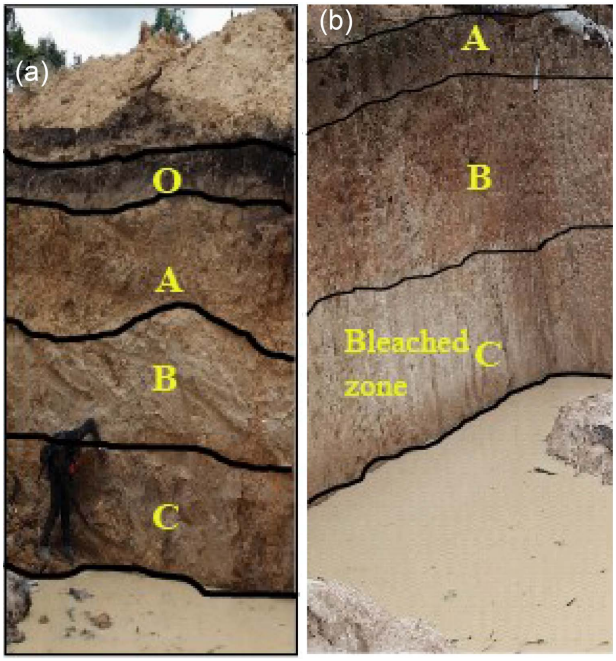

Figure 4. Soil profile at the first mining site.

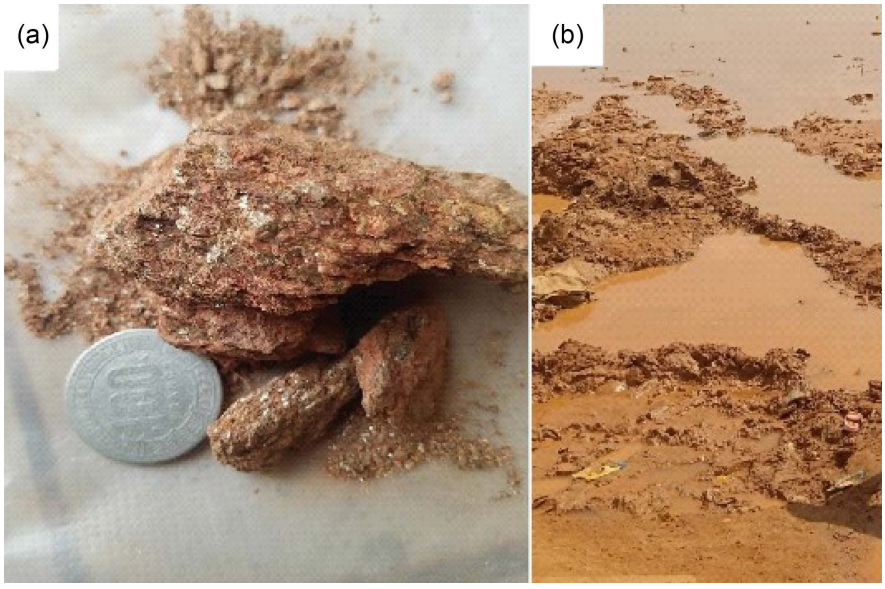

Figure 5. (a) Associated with gold in the altered granite sample; (b) and (c) watching the stream which contains gold and pyrite.

4.2. Geological Structures

4.2.1. Quartz Vein, Folding, and Foliation

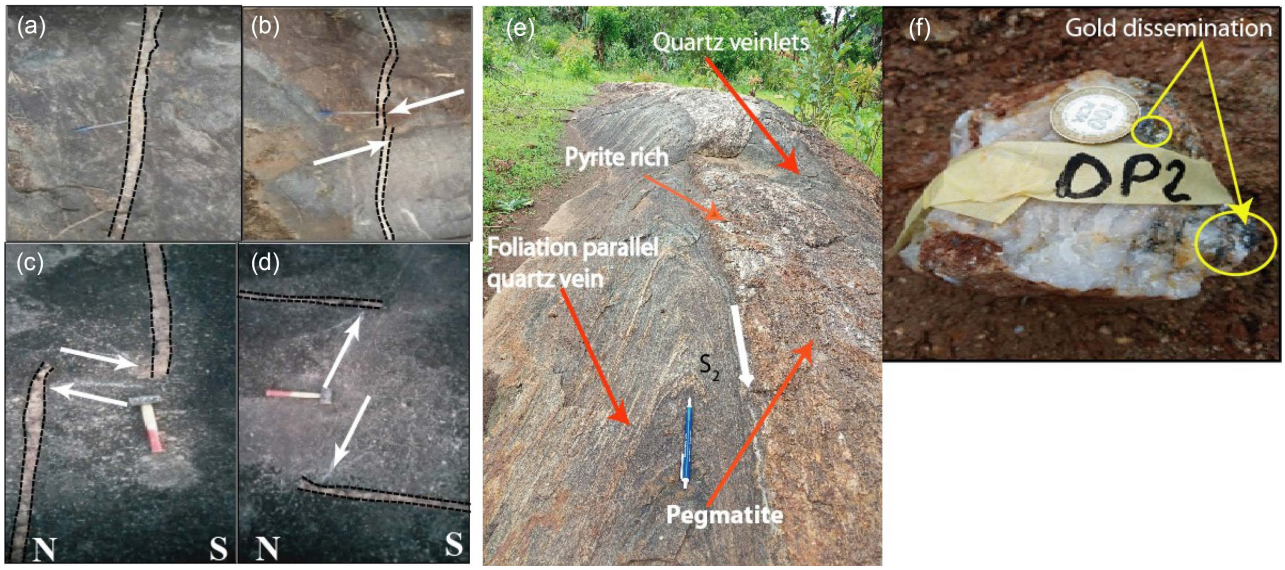

Figure 6. (a)-(c), and (d) Quartz Veins, (e) folding observed on rock outcrops and pegmatite, and (f) pegmatite sample.

The rocks in this region are characterized by their isoclinal folding, with dips typically exceeding 50˚, and a prevailing foliation orientation spanning from N-NNE to S-SSW (**Figure 6(a)**). The southern portion of the area is distinguished by the presence of extensively developed quartz veins, ranging in thickness from 3 m to 100 m and in length from 100 m to 400 m. These veins have undergone shearing and brecciation, suggesting a tectonic or metamorphic origin (**Figure 6(b)** and **Figure 6(c)**). The veins display a relatively uniform appearance across some areas, exhibiting a remarkable absence of banding, shear fractures, or analogous features. These veins have been a primary focus for local miners seeking to extract gold in the Dang Patou area. The quartz veining is predominantly associated with plutonic rocks (granitoids), though some veins are also present in metamorphic rocks. The deformed gneiss is cut by the main quartz vein, which defines the main shear plane (**Figure 6(e)**). These veins characteristically exhibit concordance with the foliation, particularly within the central part of the study area. The textures of these veins range from fine to coarse grained, with a diversity of sizes observed. Micro-sized gold particles have been documented within quartz veins, along with muscovite and pyrite. The distribution of quartz veins within the study area is illustrated in **Figure 6(a)** to **Figure 6(d)**. The mineralogical composition of the samples indicates the presence of gold, silver, copper, sphalerite, and pyrite. Gold in quartz veins is found in its native form and in association with pyrite, pyrrhotite, chalcopyrite, and magnetite. The quartz veins in this area are an epigenetic process, which suggests that quartz veins are formed during the late-stage contemporaneous deformation. In places, several parallel quartz veins form a lamination set of veins (**Figure 6(e)**). These supracrustal lithologies gneiss are intruded by the

pegmatite in the north (Figure 6(f)). The hydrothermal mineralization at Dang Patou occurs in metamorphic rocks associated with quartz veins, either parallel to the direction of foliation (Figure 6(e) and Figure 6(f)). The gold represents the latest stage of deposition in the veins or pegmatite. Many of the gold particles are of macroscopic size, with a large number visible to the eye (Figure 6(f)).

4.2.2. Digital Mapping of Structural Elements

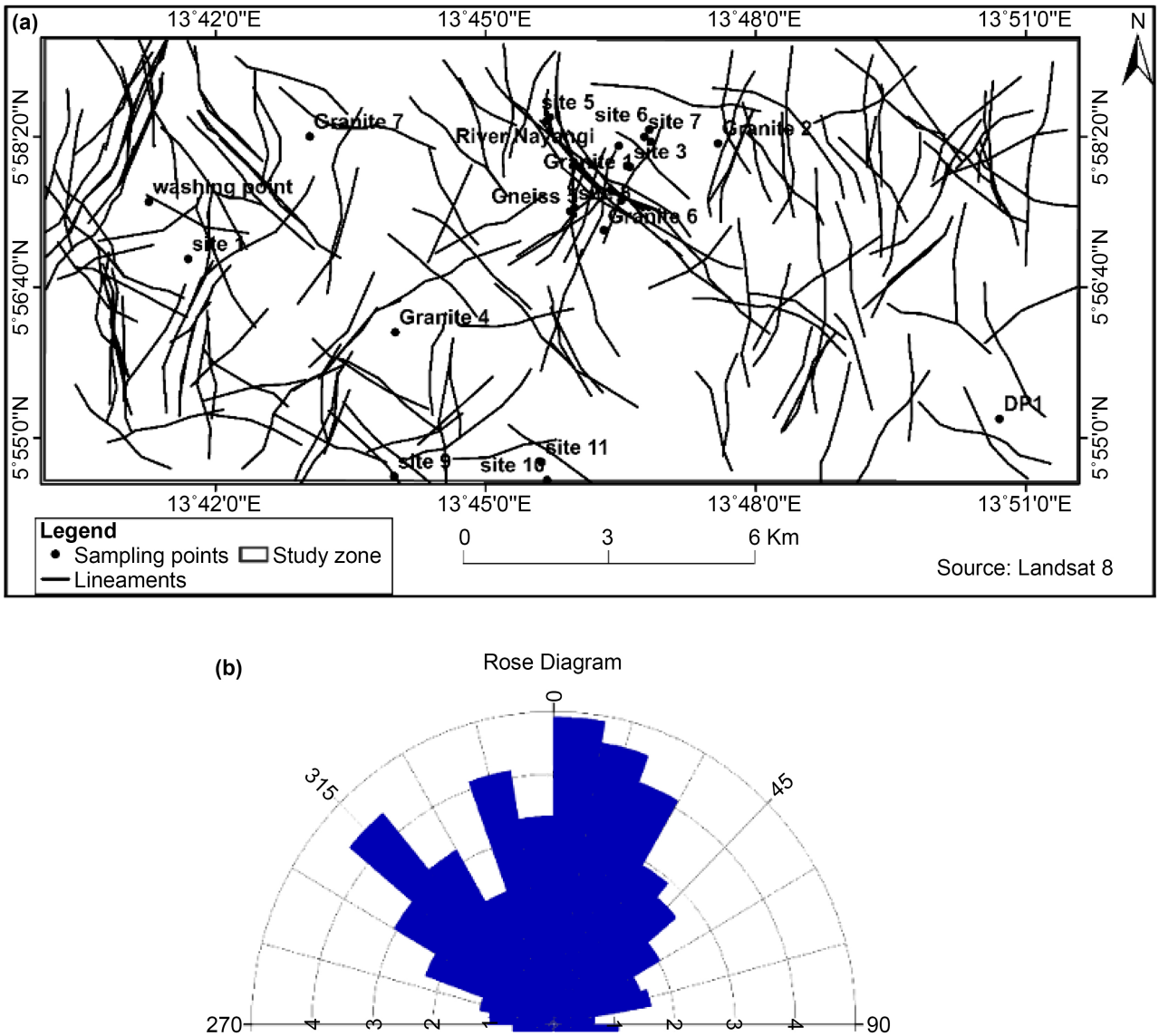

Figure 7. (a) Lineaments map and (b) rose diagram.

The lineaments were extracted in PCI Geomatica from the resulting filtered images using appropriate parameters. Lineaments may thus represent exposed faults, but also unexposed structures or crustal discontinuities whose existence is inferred from indirect sensing methods and their control on topography and magmatic activity [44]. The lineament map above is obtained from the combination

of the maxima of horizontal gradient and Euler deconvolution. Suitable lineaments greater than 2 km from the four directions were chosen and treated to realize our final lineament map (Figure 7(a)), which shows the potential mineralization zones. Four lineament directions (N-S, E-W, NE-SW, and NW-SE) extracted from PCI were superposed in GIS software (Figure 7(b)). Potential eluvial auriferous zones were identified by overlaying different data layers to identify areas with high mineral concentrations. The interpretation of Landsat lineaments (Figure 7(a)) demonstrates a broad alignment with the mapped structural framework. The analysis reveals the presence of NW-trending lineaments intersected by N-S, E-W, NE-SW, and NW-SE orientations. The NW lineaments are interpreted as distinct structural features. The majority of mineral occurrences within the Dang Patou area are located within zones of intersection between the WNW corridor and the N-S, E-W, NE-SW, and NW-SE lineaments. The lineaments are in a very similar structural position as the gold-bearing quartz vein described above. The lineament map produced from the area's fractures shows that the NE-SW direction is the primary structural orientation.

5. Structural Analysis

The structural geology and tectonic setting of hydrothermal gold deposits are critical factors in understanding their genesis and guiding exploration strategies. In gold exploitation, geologic fractures play a crucial role in the formation and concentration of gold deposits. They act as pathways for gold-bearing fluids and also as structural traps for gold accumulation. The lithology of the study area is traversed by several fractures trending from N-S to E-W. Fractures ranging from centimeters to meters were observed in several outcrops in our zone of study. The major direction of fractures observed is N53˚E (Figure 8(a)). The area's fractures show that the NE-SW is the dominant structural direction. The veinlets and veins are fracture zones strongly stained with small rounded grains distributed throughout, with their size between 2 and 5 cm (Figure 8(b)). A defining characteristic of these deposits is pronounced structural control on mineralization.

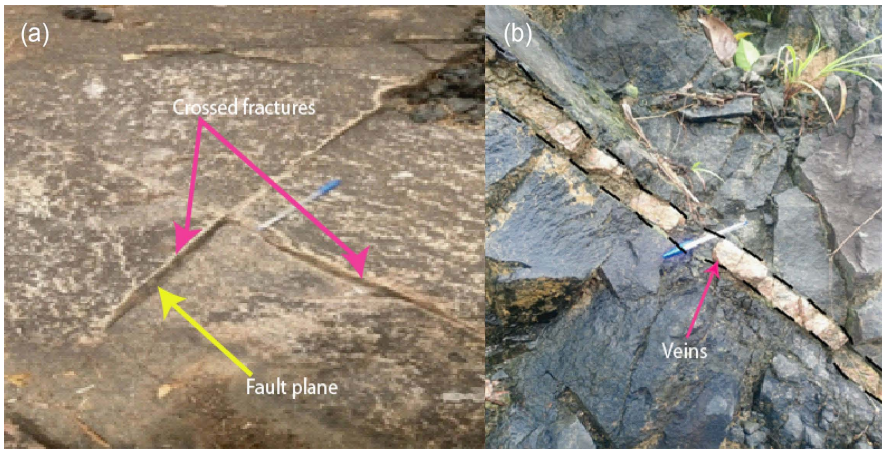

Figure 8. (a) Fractures observed on rocks, (b) veins intruded in the gneiss.

6. Mapping of Potential Mineralization Zones

The map below (Figure 9) is an assemblage of all the relevant information obtained during data collection, treatment, and interpretation. From this map, we can notice lineaments aligned with the hydrographic network and the presence of mineral indices (iron oxide, clay, and ferrous minerals) in zones of high density, confirming what was observed in the field. The area is made up of very low, low, moderate, high, and very high concentrations of lineaments. The very low concentration areas are in grey, low areas in cadet blue, moderate areas in yellow, high areas in orange, and very high areas in red, respectively. Some points correspond to old mining sites, while others correspond to points where villagers conduct small-scale artisanal mining. Already exploited zones or zones under exploitation can be seen in red, and zones not yet under exploitation in black. The geological map (Figure 9) shows that lineaments are highly concentrated on undifferentiated gneisses, as well as mineralization, explaining the traces of eluvial gold found in the field.

Images enhancing hydrothermally altered rocks using band ratios with distinctive reflection features were produced. This corresponds directly to minerals associated with this alteration and represents the surface expression of auriferous deposits. Areas with abundant iron oxide-bearing minerals (formula B4/B2), ferrous mineral indices (formula B6/B5), and clay minerals (formula B7/B5) were found using the ratio of Landsat 8 OLI band 4 over band 2. The band ratio is used to differentiate altered rocks from unaltered rocks. Using Sabin's ratio, we combined these three 4/2, 7/5, and 6/7 as RGB for lithological mapping.

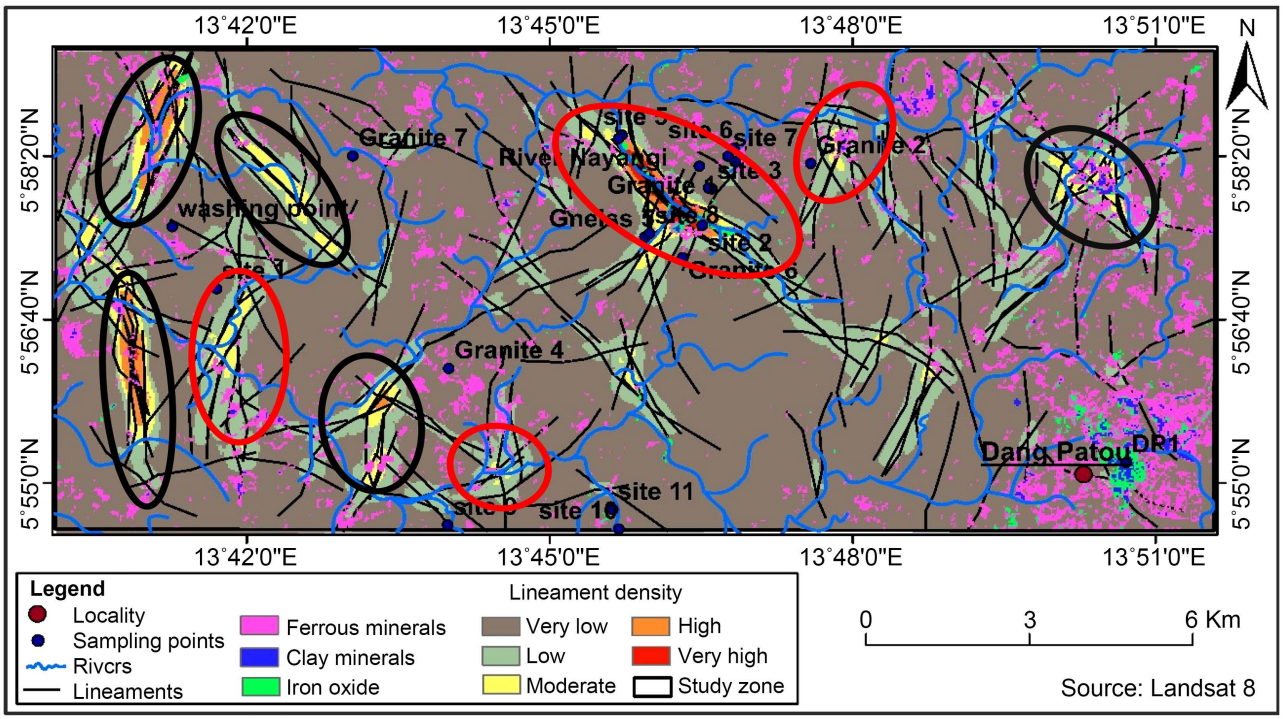

Figure 9. Potential mineralization map of the Dan Patou area showing lineament density, hydrographic network, and mineral indices.

7. Petrography

Macroscopic and microscopic analyses were conducted on plutonic igneous rocks (granites) and metamorphic rocks (gneisses) in the Dand Patou area. Several light-colored, fine-grained intrusive bodies were identified, comprising both granite and gneiss. These two facies are generally distinguishable in the field, including biotite gneiss and muscovite gneiss, though minor outcrops exhibit ambiguous similarities that may have led to misclassification. The fresh granite exhibits a gray coloration and contains rounded to ovoid phenocrysts of gray K-feldspar (up to 2 cm across) with a medium-grained matrix of quartz, orthoclase, and microperthite.

7.1. Granites

At the hand-specimen scale, the granites exhibit a porphyritic texture composed of quartz, muscovite, amphibole, biotite, orthoclase, and feldspars. Petrographic analysis reveals a coarse-grained texture dominated by primary minerals: quartz, biotite, amphibole, microcline, and plagioclase. Quartz and K-feldspar are euhedral, displaying a well-expressed equigranular texture (**Figure 10**). Thin sections show large euhedral phenocrysts of pink feldspar in a fine-grained matrix, with opaque minerals constituting the accessory phase.

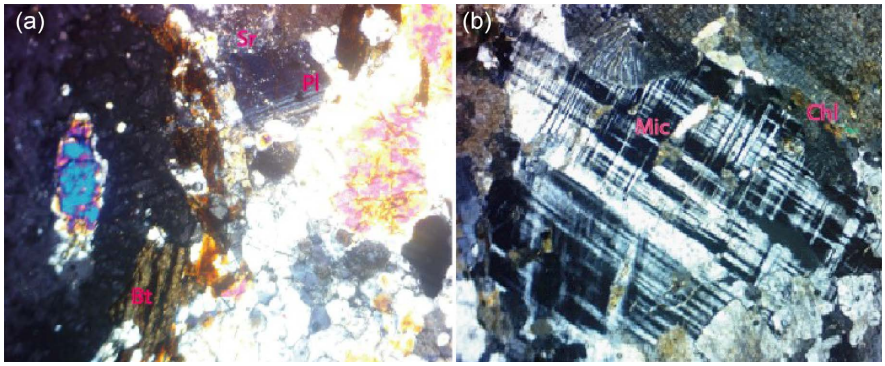

Figure 10. (a) Phenocryst of plagioclase with polysynthetic macles and sericitization; (b) Microcline and chloritization and the inclusion of biotite in microcline.

Biotite (~27 vol%), occurring as subhedral crystals (1 - 3 mm), is spatially associated with amphibole phenocrysts. Partial chloritization progresses from crystal edges toward centers in some biotite flakes. Microcline (15 vol%) occurs as 2.5 - 3.5 mm crystals. Plagioclase (20 vol%) forms large euhedral crystals exhibiting polysynthetic twinning and extensive alteration, though not destruction; sericitization and myrmekitization are observed locally (**Figure 10(a)**).

Microcline appears intergrown with plagioclase and biotite (**Figure 10(b)**), ranging from euhedral to anhedral with crystal sizes of 2.5 - 3.5 mm. Orthoclase (20 - 25 vol%) displays subhedral to anhedral morphology and low relief, dominated by crystals 1.5 mm in size and subordinate grains (0.1 0 0.9 mm). The rock exhibits characteristic plutonic texture, with total feldspar (orthoclase + microcline) estimated at 30 - 35 vol% and plagioclase at 5 - 10 vol%. Microcrysts of

biotite are included in microcline.

This medium-grained granitoid contains 5 vol% amphibole and biotite, occurring as grains and irregular flakes (≤5 mm). Biotite commonly alters to bright-green chlorite pseudomorphs containing sphene and leucoxene granules; fresh grains are muddy brown with oriented acicular inclusions. Amphibole, a minor phase, occupies interstices and fractures alongside quartz microcrystals and biotite. Accessory minerals include apatite, magnetite, zircon (trace), and sphene (partly secondary).

7.2. Gneiss

At the mesoscopic scale, gneisses display quartz, biotite, plagioclase, orthoclase, and muscovite. The rock presents a lepidoblastic texture with elongated and aligned minerals due to the action of pressure on the rock (Figure 11(a)). Interlocking quartz crystals can be observed, with hexagonal crystals of quartz developing on the quartz, feldspar content. Some exsolution textures forming myrmekites are also present. The medium-grained gneiss is composed of plagioclase, quartz, biotite, and minor hornblende, while the pegmatite is medium- to coarse-grained k-feldspar, plagioclase, quartz, muscovite, and locally biotite (Figure 11(b)). Muscovite replaces feldspar to some extent in all the granitoid leucosomes (Figure 11(c)).

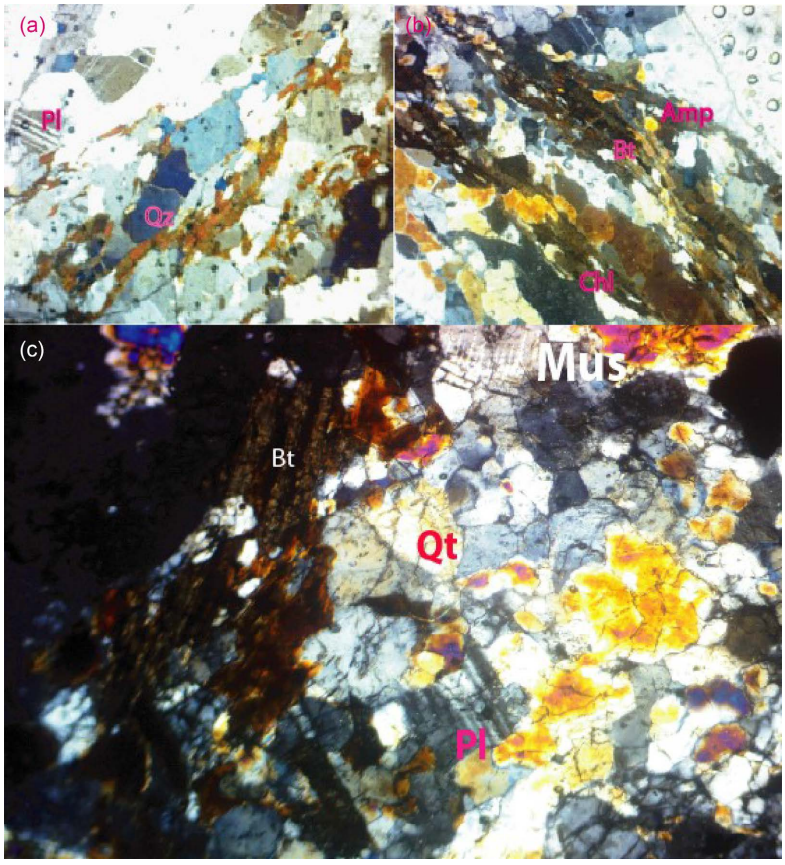

Figure 11. Lepidoblastic texture. (a) Association of muscovite and biotite, and chlorite; (b) Inclusion of biotite in microcline; (c) Muscovite replaces feldspar to some extent in all the granitoid leucosomes.

8. Discussions

The application of field, remote sensing data, and strategic prospection is a successful approach in mineral exploration and the research of mineral resources. This approach is done through the study of rock samples, their mineralogical properties, and the treatment and interpretation of remote sensing data [39]. The rocks from the study zone are rich in quartz, and some outcrops even display several quartz veins. Classification of quartz textures in epithermal vein systems has been presented by many researchers many years ago [40] [41]. Recent studies have noted that quartz textures in epithermal gold veins can provide evidence about mineralization processes [42]. The presence of a quartz vein can indicate the potential of an area to host mineralization in the surrounding rocks [42]. Folding and foliation are important geological structures that play a crucial role in the formation, concentration, and distribution of gold deposits. Folding and foliation are often associated with regional metamorphism, which can result in changes in rock composition and mineral assemblages.

Microscopic observations show that biotite and muscovite can be observed together in the same rock. Biotite in the alteration zone was altered to chlorite, and K-feldspar was altered to sericite by the sericitization process, which is the result of a mineral crystallization process that occurs in hydrous magma conditions in the liquid phase [43] [44]. The occurrence of microcline and perthite in granites and gneisses may be linked to the low temperature of metamorphism and suggests that the regional metamorphism of Adamawa has been weak in this locality.

The occurrence of quartz veins and fractures in the studied rocks indicates that during the ascent of the magma that was emplaced in the hypabyssal subsurface, the crust became domed, and fractures developed, thus providing channels for magmatic hydrothermal fluids to migrate. Gneisses from the study area are deformed and display folds and foliation, testifying to the subsequent tectonic activities along the Betaré-Oya fault. Mineral accumulation was identified in thin sections by the presence of opaque minerals, which mostly consist of heavy metals like gold, chromium, and iron, suggesting the sources of eluvial gold deposits. In the thin sections, the presence of opaque minerals included in quartz may suggest magmatic mineralization or enrichment of the rock in metallic minerals such as pyrite, chalcopyrite, and gold, which have been observed macroscopically in the rock samples from the study area. The presence of quartz veins and intrusions is a strong indicator of the post-magmatic processes responsible for mineralizing fluids. The presence of a quartz vein can indicate several important geological characteristics, such as hydrothermal activity, which generally leads to mineral concentration. These veins are excellent exploration targets and structural controls of mineralization [43]. The epigenetic nature of the quartz veins observed in this zone reflects a complex geological history encompassing hydrothermal fluid circulation, brittle deformation (fracturing and faulting), pressure-temperature fluctuations, and metasomatism.

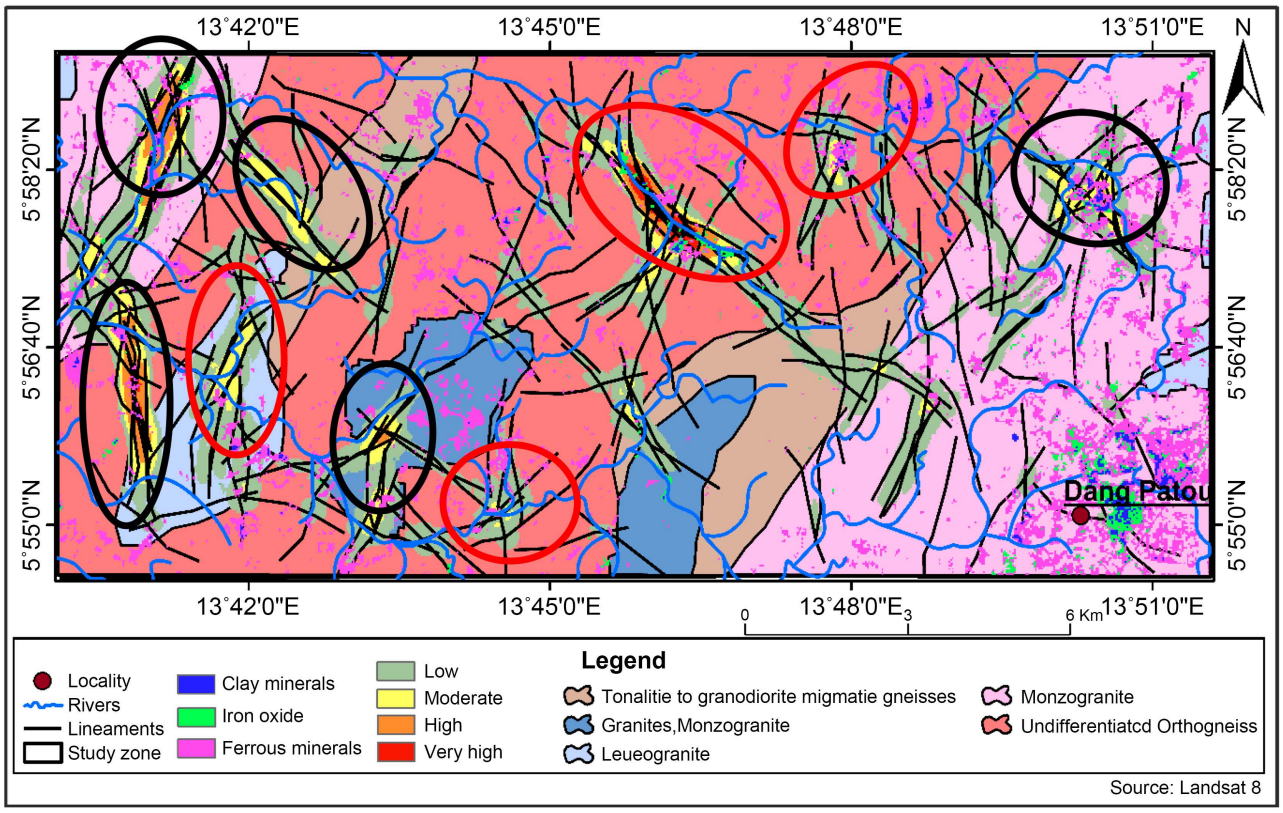

Figure 12. Geological map of the potential mineralization zone of Dang Patou.

A lineament map was the main icon used to correlate lithological formations and mineralization zones. It shows that the area has many fractures (contacts) that can be linked to the presence of mineralization zones in this area, since the exploitation carried out is from the primary source formed by the in-situ weathering of the bedrock. The identification of mineralization zones through lineaments is due to the fact that lineaments result from tectonic activities where there is an unusual accumulation of useful minerals [44]. Lineaments are generally considered as favorable zones of mineralization due to the presence of post-magmatic fluids [45]. The accumulation of useful materials in lineaments is due to constant alteration and transportation of heavy minerals by post-magmatic fluids. Post-magmatic fluids transport minerals along lineaments, and the surrounding rocks are subjected to intense alteration, hence liberating heavy minerals which arrive at the surface. Major faults and fractures that might hold minerals and have mining potential were recognized by the high lineament density [46]. The presence of an epigenetic quartz vein in granite is indicative of a complex geological history involving the circulation of hydrothermal fluids, fracturing and faulting, and pressure and temperature changes. These veins are used as pathways for mineral-rich fluids, suggesting a potential for mineral deposits within the surrounding rocks. The distribution of lineaments, particularly their intersections, has been utilized to elucidate and predict the spatial localization of magmatic and hydrothermal mineralization as documented by [47] [48]. A combination of indirect Landsat images and geo-

logical information has been used to define lineaments in Dang Patou. The relationship between these lineaments and mineralization is explored with a strong control on the gold distribution. The use of lineament intersection relationships for mineral exploration gains increased validity when defined through a multi-technique approach, such as the integration of remote sensing and geological methods. The applicability of this approach can be evaluated by incorporating known metallogenic information, which can be a guide to identify the favorable structural settings of gold deposits in the Dang Patou geological context. The geological map presented in **Figure 12** synthesizes all pertinent information derived from data collection, processing, and interpretation. Areas are color-coded to represent varying concentration levels. Very low concentrations are depicted in grey, low concentrations in cadet blue, moderate concentrations in yellow, high concentrations in orange, and very high concentrations in red.

9. Conclusion

The use of field data and remote sensing techniques in the study of the metallotectic context of Dang-Patou has proven to be a valuable approach in delimiting potential mineralization zones. The combination of data processing and fieldwork provided the geological and structural features, leading to a better understanding of identified potential gold mineralization. The field data documented herein confirm that the mineralization zone and related veins represent a structurally controlled gold-bearing quartz vein system. This approach has not only helped identify areas with high mineralization potential but also allowed for the identification of key geological controls and structures that influence the distribution of gold deposits. The petrographic characteristics and satellite minerals (pyrite, blende, chalcopyrite) and pedologic profile show different types of gold deposits (dissemination, vein, and placer). The fieldwork (petrography and structural geology) shows the potential mineralization map, which corresponds to very high, high, and moderate concentrations respectively circled in red and black. Gold exploration in the Dang-Patou is supported by the presence of two spatially associated plutonic rocks and metamorphic rocks affected by post-magmatism processes through the presence of veins and quartz veins generally accompanied by mineralizing fluids. This temporal constraint is necessary to distinguish epigenetic mineralization features from post-mineralization structures and alteration. The occurrence of pyrite, blende, and chalcopyrite in the quartz veins constitutes an indicator for researching the eluvial gold and suggests the significant role of hydrothermal fluids in the gold deposits. The combination of the geological data and the lineament map shows that the lineaments are highly concentrated on undifferentiated gneisses. This is confirmed by the presence of eluvial gold grains on some gneiss samples in the study area. The structural control of quartz veins and hydrothermal alteration, and alteration assemblages comprising mainly Bt, Qte ± Au, Pyr, indicate that the mineralization is classified as hypozonal orogenic gold class of Au deposit.

Author Contributions

Ntoumbé Mama contributed to the conceptualization, fieldwork, methodology, mapping, analysis, and writing of the article. Ntieche Benjamin participated in elaborating the methodology, mapping, and the revision of the manuscript, Mounjouohou Aziz, Amaya Adama, Nchare Mominou, and Dang Vanisa, Guihdama Dagwai contributed to mineral observation, interpretation, and reviewing the manuscript, NGounouno Ismaïla was involved in constructing the methodology, review, and analysis. All authors have read and agreed to publish this version of the manuscript.

Data Availability

The datasets generated during and/or analyzed during the current study are available from the corresponding author on reasonable request.

Conflicts of Interest

The authors declare no conflicts of interest regarding the publication of this paper.

References

[1] Vishiti, A., Suh, C.E., Lehmann, B., Shemang, E.M., Ngome, N.L.J., Nshanji, N.J., *et al.* (2017) Mineral Chemistry, Bulk Rock Geochemistry, and S-Isotope Signature of Lode-Gold Mineralization in the Bétaré Oya Gold District, Southeast Cameroon. *Geological Journal*, **53**, 2579-2596. https://doi.org/10.1002/gj.3093

[2] Toteu, S.F., Penaye, J., Deschamps, Y., Maldan, F., Nyama Atibagoua, B., BouyoHouketchang, M., *et al.* (2008) Géologie et ressources minérales du Cameroun. 33*rd International Geological Congress*, Oslo.

[3] Groves, D.I., Goldfarb, R.J., Gebre-Mariam, M., Hagemann, S.G. and Robert, F. (1998) Orogenic Gold Deposits: A Proposed Classification in the Context of Their Crustal Distribution and Relationship to Other Gold Deposit Types. *Ore Geology Reviews*, **13**, 7-27. https://doi.org/10.1016/s0169-1368(97)00012-7

[4] Barnes, S. and Lightfoot, P.C. (2005) Formation of Magmatic Nickel Sulfide Deposits and Processes Affecting Their Copper and Platinum Group Element Contents. In: Hedenquist, J.W., Thompson, J.F.H., Goldfarb, R.J. and Richards, J.P., Eds., *Economic Geology*: *One Hundredth Anniversary Volume*, Society of Economic Geologists. https://doi.org/10.5382/av100.08

[5] Candela, P.A. and Piccoli, P.M. (2005) Magmatic Processes in the Development of Porphyry-Type Ore Systems. In: Hedenquist, J.W., Thompson, J.F.H., Goldfarb, R.J. and Richards, J.P., Eds., *Economic Geology*: *One Hundredth Anniversary Volume*, Society of Economic Geologists. https://doi.org/10.5382/av100.03

[6] McOnie, A. (2006) Takitimu—Longwood Area Mineral Exploration Data and GIS Map Compilation. Ministry of Economic Development, Wellington, New Zealand Petroleum and Minerals Open File Mineral Report MR4258.

[7] Rattenbury, M.S. and Partington, G.A. (2003) Prospectivity Models and GIS Data for the Exploration of Epithermal Gold Mineralization in New Zealand. Geological and Nuclear Sciences, New Zealand.

[8] Goldfarb, R.J., Groves, D.I. and Gardoll, S. (2001) Orogenic Gold and Geologic Time: A Global Synthesis. *Ore Geology Reviews*, **18**, 1-75.

https://doi.org/10.1016/s0169-1368(01)00016-6

[9] Ntoumbé, M., Adama, A., Ntieche, B. and Nsang, F.S. (2024) Quartz Veins, Evidence of Hydrothermalism and Postmagmatic Process for Mineral Deposit Gold and Sphalerite Ore in KAAKA Area (ADAMAWA-CAMEROON). *ISAR Journal of Science and Technology*, **2**, 5-14. https://isarpublisher.com/journal/isarjst

[10] Boyle, R.W. (1979) The Geochemistry of Gold and Its Deposits. The Geological Survey of Canada Bulletins, No. 280, p. 584.

[11] Pohl, W. (1979) Metallogenic/Mineralogic Analysis Contribution to the Differentiation between Mozambiquian Basement and Pan African Superstructure in the Red Sea Region. The Geological Survey of Egypt, Vol. 9, 32-44.

[12] Sims, P.K. and James, H.L. (1984) Banded Iron-Formations of Late Proterozoic Age in the Central Eastern Desert, Egypt; Geology and Tectonic Setting. *Economic Geology*, **79**, 1777-1784. https://doi.org/10.2113/gsecongeo.79.8.1777

[13] Almond, D.C. (1984) The Concepts of Pan-African. Episode and Mozambique Belt in Relation to the Geology of East and Northeast Africa. Bulletin of the Faculty of the Earth Sciences, King Abdulaziz University, Vol. 6, 71-78.

[14] Mana, R. and Ali, R.J.R. (2002) Kerman Province Mineral Occurrence Distribution Map and Mineral Exploration Targets Area in South West of This Province Using GIS. G.I.S. Group, Geomatics Department, Tehran, Iran.

[15] Nasir, S.J. and Sankaran, R. (2017) Review of the Role of Remote Sensing Applications in Mineral Exploration and Sustainable Development in Oman. *International Journal of Environment and Sustainability*, **6**, 24-55.

[16] Sabins, F.F. (1999) Remote Sensing for Mineral Exploration. *Ore Geology Reviews*, **14**, 157-183. https://doi.org/10.1016/s0169-1368(99)00007-4

[17] van der Meer, F. (2004) Analysis of Spectral Absorption Features in Hyperspectral Imagery. *International Journal of Applied Earth Observation and Geoinformation*, **5**, 55-68. https://doi.org/10.1016/j.jag.2003.09.001

[18] van der Meer, F.D., van der Werff, H.M.A., van Ruitenbeek, F.J.A., Hecker, C.A., Bakker, W.H., Noomen, M.F., *et al.* (2012) Multi- and Hyperspectral Geologic Remote Sensing: A Review. *International Journal of Applied Earth Observation and Geoinformation*, **14**, 112-128. https://doi.org/10.1016/j.jag.2011.08.002

[19] Pour, A.B. and Hashim, M. (2015) Hydrothermal Alteration Mapping from Landsat-8 Data, Sar Cheshmeh Copper Mining District, South-Eastern Islamic Republic of Iran. *Journal of Taibah University for Science*, **9**, 155-166. https://doi.org/10.1016/j.jtusci.2014.11.008

[20] Kankeu, B., Greiling, R.O. and Nzenti, J.P. (2009) Pan-African Strike-Slip Tectonics in Eastern Cameroon—Magnetic Fabrics (AMS) and Structure in the Lom Basin and Its Gneissic Basement. *Precambrian Research*, **174**, 258-272. https://doi.org/10.1016/j.precamres.2009.08.001

[21] Freyssinet, P., Lecomte, P. and Edimo, A. (1989) Dispersion of Gold and Base Metals in the Mborguéné Lateritic Profile, East Cameroun. *Journal of Geochemical Exploration*, **32**, 99-116. https://doi.org/10.1016/0375-6742(89)90050-2

[22] Vishiti, A., Suh, C.E., Lehmann, B., Egbe, J.A. and Shemang, E.M. (2015) Gold Grade Variation and Particle Microchemistry in Exploration Pits of the Batouri Gold District, SE Cameroon. *Journal of African Earth Sciences*, **111**, 1-13. https://doi.org/10.1016/j.jafrearsci.2015.07.010

[23] Fils, S.C.N., Mimba, M.E., Nyeck, B., Nforba, M.T., Kankeu, B., Nouck, P.N. and Hell, J.V. (2020) GIS-Based Spatial Analysis of Regional-Scale Structural Controls on Gold

Mineralization along the Betare-Oya Shear Zone, Eastern Cameroon. *Natural Resources Research*, **29**, 3457-3477.

[24] Azeuda, N.K., Xie, Y.L. and Goldfarb, R.J. (2021) Gold Occurrences of the Woumbou-Colomine-Kette District, Eastern Cameroon: Ore-Forming Constraints from Petrography, SEM-CL Imagery, Fluid Inclusions, and C-O-H-S Isotopes. *Mineralium Deposita*, **57**, 1-23.

[25] Fon, A.N., Suh, C.E., Vishiti, A., Ngatcha, R.B., Ngang, T.C., Shemang, E.M., *et al.* (2021) Gold Dispersion in Tropical Weathering Profiles at the Belikombone Gold Anomaly (Bétaré Oya Gold District), East Cameroon. *Geochemistry*, **81**, Article ID: 125770. https://doi.org/10.1016/j.chemer.2021.125770

[26] Azeuda Ndonfack, K.I., Xie, Y., Goldfarb, R., Zhong, R. and Qu, Y. (2021) Genesis and Mineralization Style of Gold Occurrences of the Lower Lom Belt, Bétaré Oya District, Eastern Cameroon. *Ore Geology Reviews*, **139**, Article ID: 104586. https://doi.org/10.1016/j.oregeorev.2021.104586

[27] Gazel, J. and Gerard, G. (1954) Carte géologique de reconnaissance du Cameroun au 1/500000, feuille Batouri-Est avec notice explicative: Mémoire Direction Mines Géologie, Yaoundé, Cameroun.

[28] Toteu, S.F., Van Schmus, W.R., Penaye, J. and Nyobé, J.B. (1994) U-Pb and Sm-Nd Evidence for Eburnean and Pan-African High-Grade Metamorphism in Cratonic Rocks of Southern Cameroon. *Precambrian Research*, **108**, 45-73.

[29] Suh, C.E., Lehmann, B. and Mafany, G.T. (2006) Geology and Geochemical Aspects of Lode Gold Mineralization at Dimako-Mboscorro, SE Cameroon. *Geochemistry: Exploration, Environment, Analysis*, **6**, 295-309. https://doi.org/10.1144/1467-7873/06-110

[30] Suh, C.E. (2008) Sulphide Microchemistry and Hydrothermal Fluid Inclusion in Quartz Veins Batouri Gold District (Southern Cameroon). *Journal of the Cameroon Academy of Science*, **8**, 19-29.

[31] Abrams, M.J. and Brown, D. (1985) Silver Bell, Arizona, Porphyry Copper Test Site. Joint NASA/Geostat Test Case Study, Vol. 4, p. 73.

[32] Asaah, A.V., Zoheir, B., Lehmann, B., Frei, D., Burgess, R. and Suh, C.E. (2014) Geochemistry and Geochronology of the ~620 Ma Gold-Associated Batouri Granitoids, *Cameroon. International Geology Review*, **57**, 1485-1509. https://doi.org/10.1080/00206814.2014.951003

[33] Drury, S.A. (2001) Image Interpretation. In: Thornes, N., Ed., *Geology*, Blackwell Science, 135-158.

[34] Kemp, L.D., Bonham-Carter, G.F., Raines, G.L. and Looney, C.G. (2001) Arc-SDM: ArcView Extension for Spatial Data Modelling Using Weights of Evidence, Logistic Regression, Fuzzy Logic and Neural Network Analysis. Gological Survey of Canada.

[35] Toutin, T. (1996) Opposite Side ERS-1 SAR Stereo Mapping over Rolling Topography. *IEEE Transactions on Geoscience and Remote Sensing*, **34**, 543-549. https://doi.org/10.1109/36.485130

[36] Irons, J.R., Dwyer, J.L. and Barsi, J.A. (2012) The Next Landsat Satellite: The Landsat Data Continuity Mission. *Remote Sensing of Environment*, **122**, 11-21. https://doi.org/10.1016/j.rse.2011.08.026

[37] Roy, D.P., Wulder, M.A., Loveland, T.R., C.E., W., Allen, R.G., Anderson, M.C., *et al.* (2014) Landsat-8: Science and Product Vision for Terrestrial Global Change Research. *Remote Sensing of Environment*, **145**, 154-172. https://doi.org/10.1016/j.rse.2014.02.001

[38] Yao, T.K., Fouché-Grobla, O., Oga, M.-S.Y. and Assoma, V.T. (2012) Extraction de linéaments structuraux à partir d'images satellitaires, et estimation des biais induits, en milieu de socle précambrien métamorphisé. *Revue Télédétection*, **10**, 161-178.

[39] Anand, S.P. and Rajaram, M. (2014) Crustal Structure of Narmada-Son Lineament: An Aeromagnetic Perspective. *Earth, Planets and Space*, **56**, e9-e12. https://doi.org/10.1186/bf03352506

[40] Ramli, M.F., Yusof, N., Yusoff, M.K., Juahir, H. and Shafri, H.Z.M. (2010) Lineament Mapping and Its Application in Landslide Hazard Assessment: A Review. *Bulletin of Engineering Geology and the Environment*, **69**, 215-233. https://doi.org/10.1007/s10064-009-0255-5

[41] Prasad, A.D., Jain, K. and Gairola, A. (2013) Mapping of Lineaments and Knowledge Base Preparation Using Geomatics Techniques for Part of the Godavari and Tapi Basins, India: A Case Study. *International Journal of Computer Applications*, **70**, 39-47. https://doi.org/10.5120/11994-7875

[42] Epuh, E.E., Okolie, C.J., Daramola, O.E., Ogunlade, F.S., Oyatayo, F.J., Akinnusi, S.A., *et al.* (2020) An Integrated Lineament Extraction from Satellite Imagery and Gravity Anomaly Maps for Groundwater Exploration in the Gongola Basin. *Remote Sensing Applications: Society and Environment*, **20**, Article ID: 100346. https://doi.org/10.1016/j.rsase.2020.100346

[43] Thompson, A.J.B. and Thompson, J.F.H. (1996) Atlas of Alteration, a Field and Petrographic Guide to Hydrothermal Alteration Minerals. Geological Association of Canada, l16.

[44] Hedenquist, J.W., Arribas, R.A. and Gonzalez-Urien, E. (2000) Exploration for Epithermal Gold Deposits. *SEG Reviews*, **13**, 245-277.

[45] Partington, G.A. and Hill, M.P. (2014) Modelling of Mafic Ni-Cu-PGE and Porphyry Cu-Au Prospectivity throughout Southland, New Zealand. Eastbourne.

[46] Andarawus, Y., Likkason, O.K., Sadiq, M.A., Sani, A., Aliyu, M.K. and Anzaku, I.Y. (2024) Lineaments Characterization and Their Tectonic Significance in Mineralization Using Landsat TM Data and Field Studies along Mambilla Plateau, Northeast, Nigeria. *Dutse Journal of Pure and Applied Sciences*, **9**, 12-29. https://doi.org/10.4314/dujopas.v9i4a.2

[47] Richards, J.P. (2000) Lineaments Revisited. *SEG Discovery*, **42**, 14-20. https://doi.org/10.5382/segnews.2000-42.fea

[48] Richards, J.P., Boyce, A.J. and Pringle, M.S. (2001) Geologic Evolution of the Escondida Area, Northern Chile: A Model for Spatial and Temporal Localization of Porphyry Cu Mineralization. *Economic Geology*, **96**, 271-305. https://doi.org/10.2113/gsecongeo.96.2.271